

Shifts in light availability driven by dieback across a marsh-forest gradient

Giovanna Nordio¹  | Keryn Gedan²  | Sergio Fagherazzi¹ 

¹Earth and Environment Department,
 Boston University, Boston,
 Massachusetts, USA

²Department of Biological Sciences,
 The George Washington University,
 Washington, DC, USA

Correspondence

Giovanna Nordio
 Email: nordiog@bu.edu

Funding information

USA National Science Foundation,
 Grant/Award Numbers: 1832221, 2012322

Handling Editor: Charles D. Canham

Abstract

Ecological zonation in coastal forests is driven by sea level rise and storm-surge events. Mature trees that can survive moderately saline conditions show signs of stress when soil salinity increases above its tolerance levels. As leaf burn, foliar damage, and defoliation reduce tree canopy cover, light gaps form within the crown. At the forest-marsh edge, canopy cover loss is most severe; trunks of dead trees without canopies form “ghost forests.” Canopy thinning and light from the edge alter conditions for understory vegetation, promoting the growth of shrubs and facilitating establishment and spread of invasive species that were previously limited by light competition. In this research, we present an analysis of illuminance and temperature in a coastal forest transitioning to a salt marsh. Light sensors above the ground surface were used to measure light attenuation of trees and understory vegetation and to observe the effect of reduced canopies at the forest-marsh edge. Farther from the marsh, where salinity is lower and trees are healthy, dense canopies attenuate light. We estimate that during the growing season, tree canopies intercept 50% of illuminance on average. Closer to the marsh, canopy thinning, and tree death allow greater light penetration from above, as well as from the adjacent marsh. These illuminance values are further increased by light penetration from the forest-marsh edge (edge effect). Here, higher illuminance may permit *Phragmites australis* expansion. At intermediate locations, trees intercept between 32% and 49% of light and the understory shrub *Morella cerifera* intercepts a further 45% of penetrating light based on comparisons of illuminance above and below shrub canopies. Light penetration from the edge can also be felt. The presence of *M. cerifera* reduces the air temperature close to the soil surface, creating a cooler summer microclimate. The tree health state is reflected in the canopy size. The canopy patterns and the edge effect are responsible for light availability distribution along forest-marsh gradients, consequently affecting the understory vegetation biomass. We conclude that during forest retreat driven by sea level rise, tree dieback increases light availability favoring the temporary encroachment of *Ph. australis* and *M. cerifera* in the understory.

This is an open access article under the terms of the [Creative Commons Attribution License](#), which permits use, distribution and reproduction in any medium, provided the original work is properly cited.

© 2024 The Author(s). *Ecosphere* published by Wiley Periodicals LLC on behalf of The Ecological Society of America.

KEY WORDS

coastal forest retreat, edge effects, illuminance, invasive species, salinization, temperature

INTRODUCTION

Sea level rise and storm surges are the main drivers of coastal forest retreat and consequent marsh expansion (Desantis et al., 2007; Doyle et al., 2010; Fagherazzi et al., 2019; Kearney et al., 2019; Kirwan & Gedan, 2019; Schieder & Kirwan, 2019; Tully et al., 2019; Nordio et al. 2023). Salinization results in the mortality of trees and emergence of ghost forests. Trees dieback triggers major changes in light regime as coastal forest transitions to salt marsh. Changes in the light availability of salt-stressed forests have been little studied in comparison with variations in soil salinity. However, these changes have important effects on understory vegetation establishment and growth that may determine ephemeral or long-lasting stages of transition through ecological dynamics such as priority effects.

Trees affected by salinization and flooding show clear signs of stress. High salinity can cause leaf burn, foliar damage, defoliation, and tree mortality (Kotuby-Amacher et al., 2000). In flooded and high-salinity conditions, when soil water potential drastically decreases, trees reduce carbon assimilation, stomatal conductance, and consequently their photosynthetic activity (Antonellini & Mollema, 2010; Johnson & Young, 1993; Munns & Tester, 2008; Pezeshki, 1992; Poulter et al., 2008; Williams et al., 1999; McDowell et al. 2022). Seedling and germination stages are the most sensitive to salinization and flooding events (Woods et al., 2020). Frequent flooding and salinization eventually kill mature trees generating new patterns in the canopy openness, although different tree species exhibit different salinity tolerance levels (Conner et al., 2007).

Forest gap formation and light availability in non-salt-stressed forests have been widely documented in previous studies, for example (Beaudet et al., 2004; Canham, 1988; Canham et al., 1990, 1994, 1999; Comeau, 2000; Duursma & Mäkelä, 2007; Lieffers et al., 1999; Montgomery & Chazdon, 2001; Ni et al., 1997; Nicotra et al., 1999; Rissanen et al., 2019; Rosema et al., 1992; Stenberg, 1996; Tang et al., 2019; Whitmore, 1989). Canopy gaps are preferential ways for radiation penetration, and even in very dense forests, light penetration through the canopy (sum of diffusive and direct radiation) is around 2% (Canham et al., 1990). Gaps provide microenvironmental conditions in terms of light, water content, and temperature, favoring the establishment of shade intolerant species (Yamamoto, 2000).

Plants growing in forests stressed by flooding and salinization respond to changes in the light regime that

occur as the canopy opens. Canopy openness and light transmittance strongly correlate with understory species richness, suggesting that light availability is among the main drivers of biodiversity in such environments (Dormann et al., 2020; Walters et al., 2021). Exotic plant species can quickly encroach, diversifying the *in situ* biodiversity. For example, *Phragmites australis* is among the first invaders, arriving before native salt marsh species (Carr et al., 2020; Shaw et al., 2022; Smith, 2013). Dense understory vegetation can also limit light transmittance to the ground surface, slowing additional vegetation growth (Beaudet et al., 2004).

Typically, higher light availability is present along a forest edge (Delgado et al., 2007; Pohlman et al., 2007). In tropical forests adjacent to creeks, light intensity is high in comparison with forests adjacent to anthropogenic edges, and the edge effect extended 50 m into the forest (Pohlman et al., 2007). Delgado et al. (2007) showed that between 70% and 96% of the total light received at a forest edge was filtered at 100 m in the interior of a laurel and pine forest. In the case of salt-stressed forests, reduced canopies at the forest-marsh edge enhance lateral light penetration, and higher light conditions can occur at a greater distance from the forest edge than in a typical forest. This extended edge effect may be beneficial for some species at specific locations. For example, greater light availability was considered beneficial for mature trees at the forest-marsh ecotone in coastal forests along the Long Island Sound, where tree growth at the edge exceeded that of the forest interior (Field et al., 2016). Positive effects may also be ephemeral, resulting in higher growth of trees that ultimately become stressed and die, as ghost forests expand (Haaf et al., 2021).

At the forest edges, higher temperature values were also detected (Delgado et al., 2007; Pohlman et al., 2007). Pohlman et al. (2007) measured a temperature increase near the soil of 2°C in a forest-highway edge in the Wet Tropics World Heritage Area of northeastern Queensland, Australia. Where the salinity values are higher, high temperatures worsen soil conditions and the photosynthetic response of native trees by increasing evaporation (Jolly et al., 1993; Munns & Tester, 2008). The effects of temperature can be weakened by canopy shading, both for overstory and understory vegetation. Canopy shading was found to be beneficial to limit evapotranspiration (Raz-Yaseef et al., 2010). A change in canopy cover from 10% to 100% would decrease soil evaporation from 150 to 86 mm/year. Understory vegetation

mitigates temperature effects as well, establishing new microclimate conditions (D'Odorico et al., 2010, 2013; Huang et al., 2018; Stickley & Fraterrigo, 2021). Shrubs also reduce cold induced mortality, making the understory temperature conditions warmer (Huang et al., 2018).

As far as we know, few studies have focused on estimating light availability in coastal forests affected by sea level rise. Walters et al. (2021) used light sensors to detect illuminance values in a marshland/forest continuum, where a portion of the forest was experimentally clear-cut. Zhu et al. (2003) used hemispherical images to estimate direct and diffuse light in coastal forested areas affected by thinning treatments. Here, we present illuminance and temperature data collected in a coastal forest in Virginia, USA, and compare light availability between different ecological stages of forest dieback. We compare light data with ecological parameters at the site to determine how light penetration is affected by damage in the forest canopy caused by salt-stress, as well as by the resulting variations in forest understory vegetation structure. Moreover, we shed light on the edge effects driven by light entering from the forest-marsh boundary and their link with the new establishing vegetation.

STUDY AREA

Our research focuses on a coastal forest bordering a salt marsh in Nassawadox, Delmarva Peninsula (VA, USA) (Figure 1). The forest covers a 3-ha area with an average

elevation of 1 m on NAVD88 (North America Vertical Datum) and a distance from the salt marsh ranging from 100 to 300 m. The forest is dominated by loblolly pines (*Pinus taeda*) that, depending on their distance from the salt marsh, are more or less affected by salinization and flooding events. Where these events are less intense and less frequent, trees do not show apparent signs of stress in their canopies. We observationally divided the forest into three zones: (1) low forest, the closest to the marsh, is characterized by barren or dead trees, and *Phragmites australis* is the dominant understory species; (2) mid-forest, at a distance of around 150 m from the forest-marsh boundary, where trees and shrubs (*Morella cerifera*) coexist, and gaps in the forest canopy are present caused by occasional dead trees or fallen branches; and (3) high forest, at a distance of 300 m from the forest-marsh boundary, where healthy trees are present with a dense canopy. Six different forested sites are considered in the analysis. Two in the high forest, H5 and H7; two in the mid-forest, M1 and M2; and two in the low forest, L1 and L6 (Figure 1b).

DATA AND METHODS

Light data

Illuminance (lumens per square meter) and temperature (in degrees Celsius) data were collected every two hours

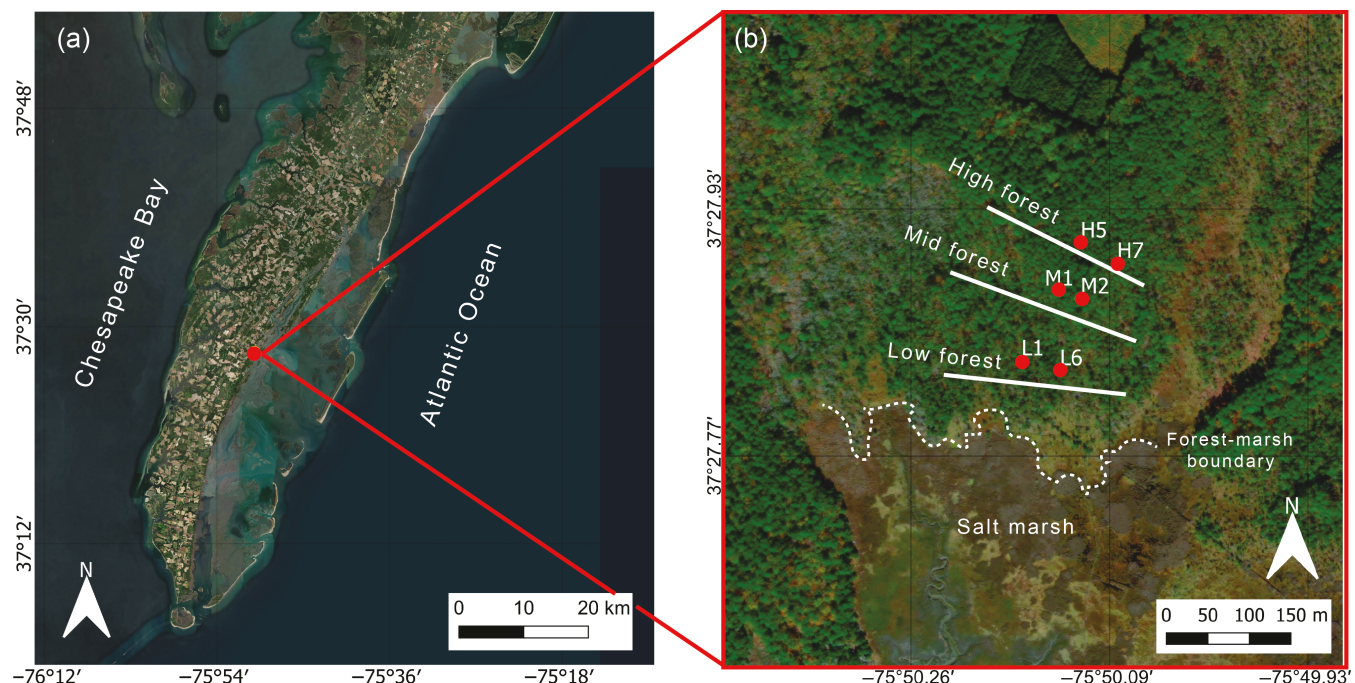


FIGURE 1 (a) Study area and (b) the different ecological zones in the coastal forest. Images from ESRI (Environmental System Research Institute) Satellite Imagery (March 3, 2013).

at each site from June 2021 to May 2022. These data can be found in the VCR-LTER (Virginia Coast Reserve-Long Term Ecological Research) portal (ID: VCR22344) (Fagherazzi & Nordio, 2022; Nordio & Fagherazzi, 2022). For each site, four HOBO pendant sensors by ONSET were installed on two poles. Two sensors at 30 cm (low sensors) and 2 m (high sensors) were fixed perpendicularly to the pole through two brackets. The brackets were oriented toward the south. The pole locations at each site were chosen according to two criteria: (1) representative of the in situ ecology and (2) open to ambient light penetration (i.e., not too close to trees or tall shrubs). The poles were called using the site name and the subscription _1 and _2 to characterize the pole 1 and the pole 2 in the same forested areas (for instance in H5: H5_1 and H5_2). Photos of the locations of the poles taken in May 2022 are shown in Appendix S1: Figures S1–S3. The illuminance and temperature data were first filtered to daylight hours between 10:00 am to 4:00 pm. This allowed comparison of the mean of the maximum values reached during the day, emphasizing inter-site differences. An analysis with all values would risk homogenizing the data, since no or very low illuminance is detected outside of these hours.

HOBO light sensors were chosen because they are inexpensive, easy to use, and able to collect both temperature and illuminance values (Long et al., 2012). Their reduced size and price make them a good choice in an environment affected by storm-surge events and strong gusts that threaten the instruments functioning. Illuminance values collected by these sensors are the sum of the sky radiation components, the downward reflected beam radiation, and the transmitted beam radiation (Hutchison & Matt, 1976). Moreover, illuminance measurements directly collected by each sensor, rather than photosynthetic active radiation (PAR), were sufficient for sites comparison, according to the procedure followed by Walters et al. (2021). Below-canopy illuminance measurements were compared with radiation values collected at VCR-LTER Oyster station (OYSMET) and reported in the VCR-LTER portal dataset (ID: VCR97018) (Porter et al., 2022) to estimate tree canopy attenuation. At this station, radiation was measured in an open space, free from obstacles, and it is considered herein as a proxy for the radiation that reached the top of the canopy. Radiation was converted to illuminance according to Michael et al. (2020).

The filtered data were daily averaged, and values from cloudy days were removed from the dataset. Cloudy days were identified using Visual Crossing-Weather data portal in the weather stations around Nassawadox (VA). We excluded from the analysis days during which the cloud percentage was higher than 50%. Clouds modulate

surface solar radiation in a very complex manner depending on clouds type. Gu et al. (2001) found that cloud cover triggers a twofold effect on surface irradiance with a 50% attenuation and a 14% enhancement by scattering and diffusion. The average duration of enhancement periods was about 1/3 of the average duration of attenuation periods. This brief time is sufficient to affect chemical processes but not necessarily the stomata response. Due to this complexity, we decided to filter the data based on cloud cover.

Ecological data

Light data were coupled with ecological data collected in 2021 and 2022 and reported in the VCR-LTER portal dataset (ID: VCR22354) (Gedan et al., 2021) (Table 1). Trees greater than 5 cm dbh were censused inside 20 × 20m plots in each forest site (Gedan et al., 2021). For each tree, DBH was measured at 1.37 m from the tree base. Basal area, considered the most significant variable describing the difference between forest stages, was then calculated. In the high forest 91%–95% of the basal area consisted of *Pi. taeda* species, in the mid-forest around 78%–82% and in the low forest 34%–57%. In this latter, *Juniperus virginiana* is the other dominant species (Gedan et al., 2021). Tree health was also ranked on a 0–10 scale based on canopy integrity, where 0 signifies a dead tree and 10 a perfectly full canopy. Regardless of tree species, the average basal area (in square meters per hectare) of healthy trees (i.e., health score >6, with only partial signs of stress) was considered in the analysis. Tree data were integrated with tree leaf area index (LAI) measurements. LAI data were collected between May 2021 and May 2022 using LAI-2200C Plant Canopy Analyzer (LI-COR, Lincoln, NE). For each month, three measurements were taken directly above the center of each study site, recording tree canopy LAI. A monthly mean for high-, mid-, and low-forest sites was considered in the next analysis. Shrub species were identified in a 2-m-radius circle around the center of each site (Gedan et al., 2021). We concentrated on the dominant species *M. cerifera*, which constituted 99% of all shrubs recorded. Shrub basal area, height, and canopy width were recorded. In 2022, canopy width at 1 m from ground surface and number of stems of *M. cerifera* were measured in a circular area of 5-m diameter around each sensor pole and used to calculate coverage (in square meters per hectare) (Table 1; Appendix S1: Figures S1–S3). In 2022, trees, *M. cerifera* shrubs and invasive vegetation stems were counted in a circular area of 5 m diameter around each sensor pole (Table 1; Appendix S1: Figures S1–S3). We concentrated our analysis on the *Ph. australis* species,

TABLE 1 Vegetation data (number of individuals) in a 5-m radius around each sensor.

Site	Pole ID	<i>Morella cerifera</i>	Trees (all species)	<i>Phragmites australis</i>
H5	H5_1	7	0	0
	H5_2	15	0	0
H7	H7_1	8	1	22
	H7_2	3	3	128
M1	M1_1	31	1	13
	M1_2	10	6	0
M2	M2_1	11	2	317
	M2_2	14	3	0
L1	L1_1	0	3	630
	L1_2	0	0	555
L6	L6_1	0	3	78
	L6_2	0	3	381

the most dominant invasive vegetation that first invades the stressed forests and precedes marsh expansion. Average density of the *Ph. australis* stems (in numbers per square meter) was finally computed.

In addition, biomass of understory vegetation (*M. cerifera* and *Ph. australis*) was calculated using published allometric equations. *M. cerifera* biomass was estimated using the Sah et al. (2004) equation, with crown area and stem height as independent variables. Crown area was calculated as circular and considering the average canopy width at 1 m height. This latter variable and an average stem height at each site was calculated from data collected by Gedan et al. (2021) and used in the equation. *Ph. australis* biomass was calculated using the Kauppi et al. (1983) equation, using stem height as the independent variable. From observations in the field, average *Ph. australis* height was 1.80 m at these sites.

Statistical approach

Illuminance and temperature data collected at 2 m and 30 cm above the ground surface were daily averaged. Data from H5 and H7 were combined to represent the high forest, M1 and M2 to identify the mid-forest and L1 and L6 the low forest. One-way ANOVA and post hoc Tukey test (95% confidence level) were used to test for differences between high-, mid-, and low-forest illuminance and temperature values for each month. According to Nicotra et al. (1999), the autocorrelation between light measurements ceases to be significant at an inter-plot distance of 20 m. Becker and Smith (1990) determined that in a tropical wet forest, the spatial autocorrelation

between solar radiation measurements is low for distances between 2.5 and 22.5 m depending on season. Other ecological studies suggest a 5–10-m threshold for inter-plot distance in order to consider the data independent (Becker & Smith, 1990; Dale & Fortin, 2009; Wagner & Fortin, 2005). Our sensors were more than 20 m apart so that illuminance and temperature can be considered independent, satisfying the main assumption for the ANOVA test. Using illuminance values calculated at the top of the tree canopy, we measured light attenuation at 2 m, representing the tree canopy effect, and 30 cm, representing the understory vegetation effect, and reported the results for each season. Solar altitude angles were correlated with mean illuminance values for each month to better compare light dynamics in the different forested areas. Mean monthly solar altitude angle (considering data between 10:00 am and 4:00 pm) was calculated from the mean latitude of the study site (ϕ), the solar declination angle (δ), and the mean hour angle (γ) between 10:00 am and 12:00 pm, with $\gamma = 2\pi t/24$ (where t are hours after solar noon), according to the equation $\cos\theta = \sin\phi\sin\delta + \cos\phi\cos\delta\cos\gamma$ (Monteith & Unsworth, 2013). The correlation between solar angle and canopy attenuation due to trees or shrubs was then studied. Mean illuminance values were compared with ecological parameters averaged by forest level: tree LAI, tree basal area (in square meters per hectare), *M. cerifera* coverage (in square meters per hectare), and *Ph. australis* density (in numbers per square meter). Finally, linear regression analyses were conducted with temperature and illuminance as predictors and understory biomass (in grams per square meter) as response variable. Since four independent hypotheses were tested, Bonferroni's correction was used. The original significant level α of

0.05 is therefore corrected at 0.0125 for the tests (α /number of independent tests).

RESULTS

Illuminance and temperature trends

Monthly illuminance and temperature measured in high, mid-, and low forest vary considerably throughout the year (Figures 2 and 3). In the high sensors, the illuminance values significantly differed among sites ($p < 0.05$) and presented high variance from June to August and in April. Maximum median illuminance in the high sensors was reached in July with $50,000 \text{ lm/m}^2$ in the high forest, $65,000 \text{ lm/m}^2$ in the mid-forest, and $110,000 \text{ lm/m}^2$ in the low forest. In the same month, the illuminance values measured by the low sensors were quite similar. During winter and fall, illuminance decreased, and consequently so did the difference among the three sites (Figure 2a). Illuminance values measured at the low sensors suggested a similar trend. During summer and spring, illuminance in the low forest was significantly higher than in the other forest levels ($p < 0.05$). During winter and fall, illuminance values in the mid-forest were significantly lower than those reached in the other levels ($p < 0.05$) (Figure 2b). In this period, the median illuminance measured in the low sensors, around $10,000 \text{ lm/m}^2$, was on average half the illuminance measured with the high sensors. Temperatures measured by low sensors in the mid-forest tended to be always lower than in the other forest levels (Figure 3b). In particular, they were on average 4% and 6.5% lower than high- and low-level sensors, respectively. During summer and spring, temperatures in the low forest sites, collected with both high and low sensors, were significantly higher than those in the other sites (Figure 3). As with illuminance, differences in temperature were reduced in winter and fall. Although illuminance was overall more variable across the seasons and differed more among forested sites than temperatures, temperature was highly correlated with the illuminance measured by the high sensors ($R^2 > 0.75$, $p < 0.5$ not shown here).

All forest levels displayed illuminance attenuation by the forest canopy. The largest attenuation was measured in the high forest, at about 50%. In the low forest, illuminance attenuation was around 25% during the summer season (Figure 4a). Illuminance attenuation due to understory vegetation reached maximum values in each forested area in fall. Over the seasons, illuminance attenuation due to understory vegetation is higher in the mid- and low forests than in the high forest. During summer, understory vegetation in the low forest attenuated

illuminance from the high sensors more than in other seasons (Figure 4b). During the other seasons, illuminance attenuation by understory vegetation was higher in the mid-forest.

Correlation between illuminance and angle of solar radiation

Correlations between monthly mean illuminance and monthly mean solar altitude angles are shown in Figure 5. When solar angles were low, illuminance values in the high sensors were similar in the three forest levels (Figure 5a). When solar angles were high, illuminance values tended to be significantly different among the high, mid-, and low forests. A critical solar altitude angle $\theta_{\text{crit}} = 43^\circ$ was identified. For angles higher than this value, mean monthly illuminance values measured in the three forested areas diverge. In particular, when solar elevation angles are higher than θ_{crit} , illuminance was significantly greater ($p < 0.05$, *t* test result) in the low forest than the high forest. This difference is supposed to be driven by higher canopy attenuation in the high forest during the growing season and edge effects felt in the low forest. For values lower than θ_{crit} , illuminance measured with the low sensors in the mid-forest was always lower than illuminance in the high and low forest (Figure 5b), as a result of shrub canopy attenuation. In mid-forest sites, where the estimated shrub biomass of *Morella* was higher compared with *Ph. australis* (M1_1, M1_2, M2_2; Table 1), the difference in illuminance values between high and low sensors was correlated with solar angles lower than θ_{crit} (Figure 5c). As a result, as solar altitude angles increased, the difference in illuminance between high and low sensors significantly increased (Figure 5c).

Illuminance and vegetation

Average illuminance was related to ecological parameters collected in summer 2021 (Figure 6). The largest basal area of healthy trees was measured in the high forest, where mean illuminance values were $40,000 \text{ lm/m}^2$ on average. The lowest values of tree basal area were measured in the low forest, where illuminance values in the high sensors were maximum, reaching about $60,000 \text{ lm/m}^2$ (Figure 6a). A similar correlation can be seen between illuminance values and monthly LAI (Figure 6b). In the high forest, higher LAI values around 1.7 were linked to lower illuminance in the high sensors, while significantly lower LAI values in the low forest of 0.88, were linked to higher illuminance values. LAI values detected in the high and mid-forest were not significantly different. Figure 6c

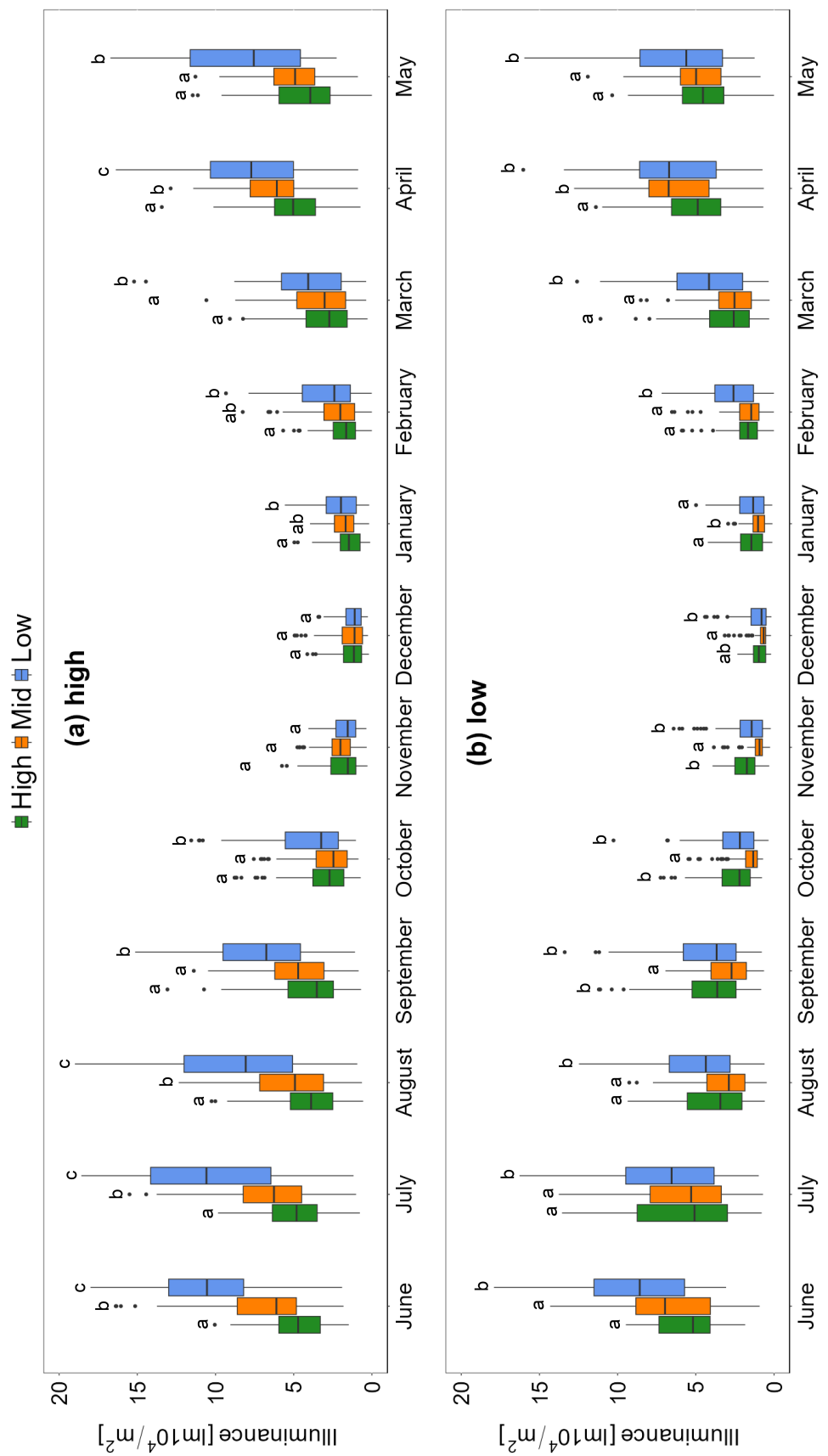


FIGURE 2 Daily averaged illuminance values over the months in high, mid-, and low forests in (a) high sensors and (b) low sensors. Illuminance values collected for both poles in H5 and H7 are combined to represent the high forest, M1 and M2 to represent the mid-forest and L1 and L6 to represent the low forest. In the boxplot, the lower boundary of the box represents the first quartile (Q1), the midline within the box indicates the median (Q2), and the upper boundary of the box corresponds to the third quartile (Q3). This means that 50% of the data points lie within the interquartile range, which is the range between Q1 and Q3. The whiskers extend to the minimum and maximum values within the dataset, excluding any outliers. The solid datapoints outside the whiskers represent outliers. The letters above each boxplot denote the results of a post hoc Tukey test, indicating significant differences between zone categories for each month.

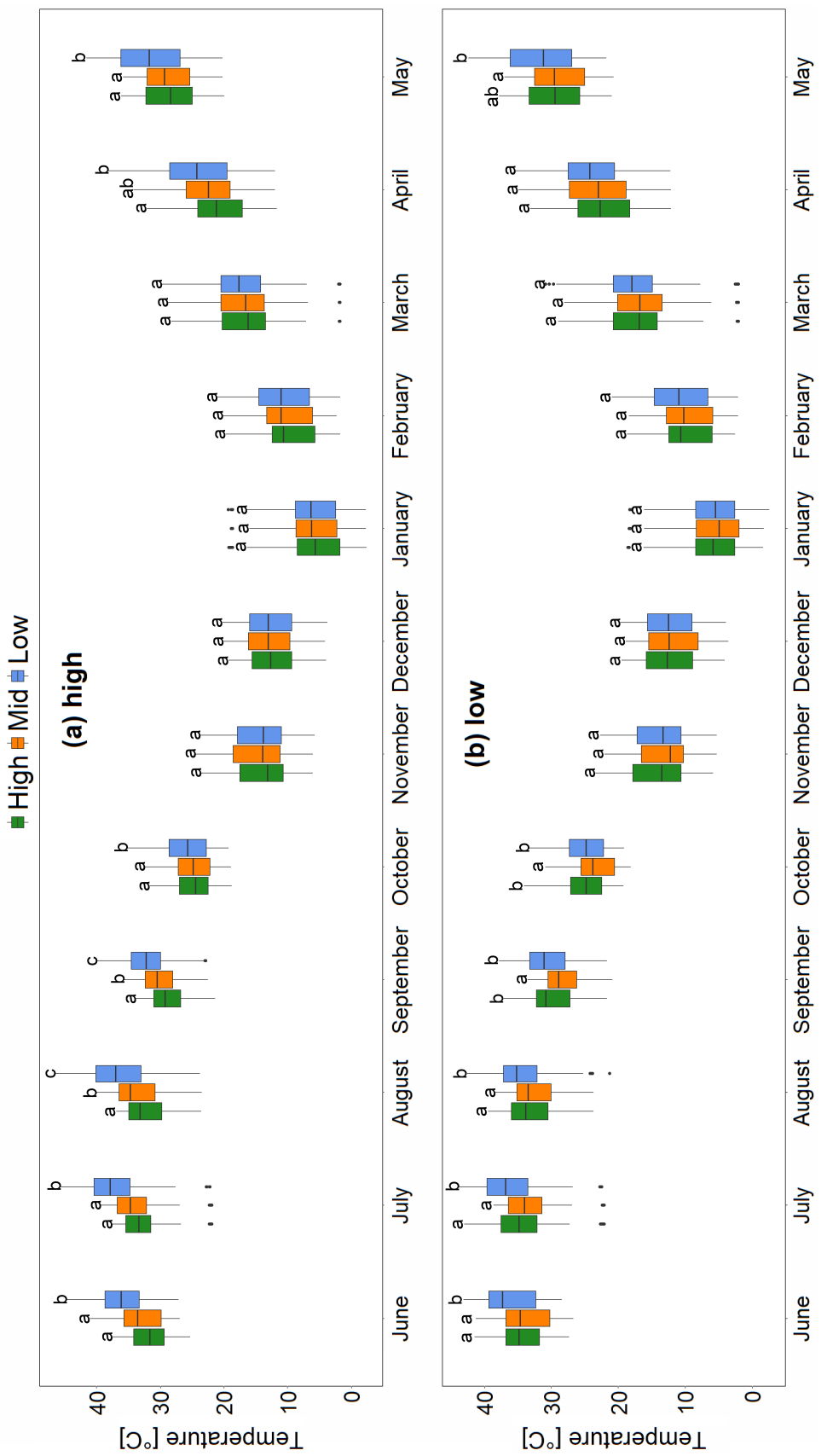


FIGURE 3 Daily averaged temperature values over the months in high, mid-, and low forests in (a) high forests and (b) low forests. See Figure 2 caption for details.

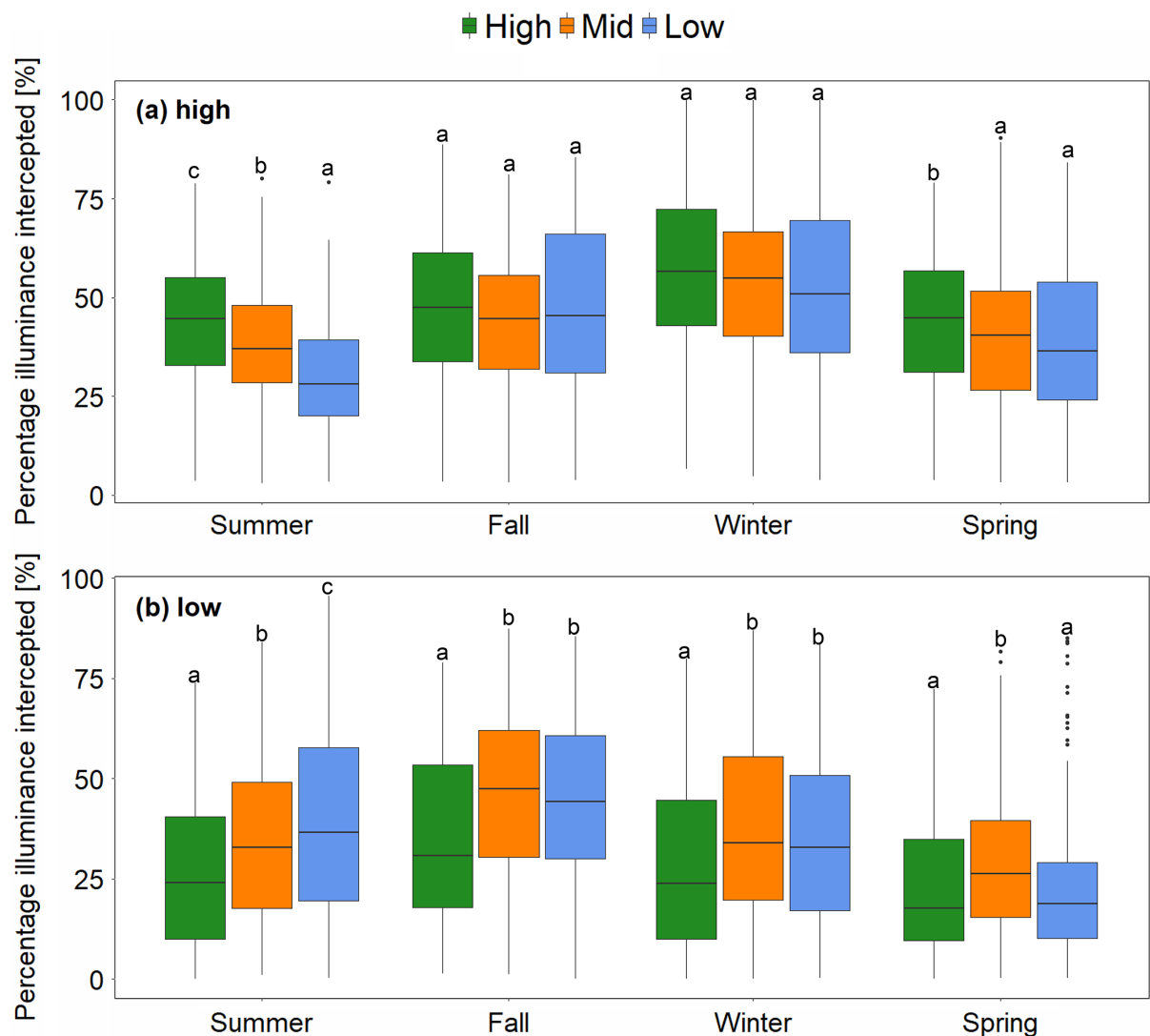


FIGURE 4 Daily averaged illuminance attenuation over the seasons in high, mid-, and low forests from (a) top of the canopy to high sensor and (b) high sensor to low sensor. The letters above each boxplot denote the results of a post hoc Tukey test, indicating significant differences between zone categories for each season. See Figure 2 caption for further details.

suggests that *M. cerifera* shrubs affect the average illuminance values measured in the low sensors in the mid-forest sites. High illuminance values measured by the high sensors of the low forest sites promote a high density of *Ph. australis* (Figure 6d). In fact, in the low forest sites, *Ph. australis* density reached a maximum of 21.5 stems/m², whereas in the high and mid-forests, where illuminance values were low, *Phragmites* density was between 3 and 5 stems/m².

Additional analysis to relate the biomass of understory vegetation for each site with abiotic conditions of temperature and illuminance is shown in Figure 7. Linear regression analysis, with average illuminance and temperature as independent variables, significantly explained biomass, whether high or low sensor measurements were used as the predictor variables ($R^2 > 0.5$,

$p < 0.0125$) (Figure 7). Biomass and temperature in the low sensors were the least correlated with $R^2 = 0.48$ and $p = 0.0125$ (Figure 7a). Even if temperature and illuminance values correlated with one another (not shown; $R^2 > 0.6$, $p < 0.0125$), the illuminance-biomass and temperature-biomass relationships allow to better investigate the attenuation effects of the trees and understory vegetation.

From Figure 7a,c we can recognize how vegetation affects illuminance and temperature. In the mid-forest sites M1 and M2, the high percentage coverage of *M. cerifera* reduces both illuminance and temperature measured by the low sensors. This effect is also evident in the biomass-temperature relationship for the low sensors (Figure 7a). For instance, M2 had a high density of both *M. cerifera* and *Ph. australis* stems. Here, even if the

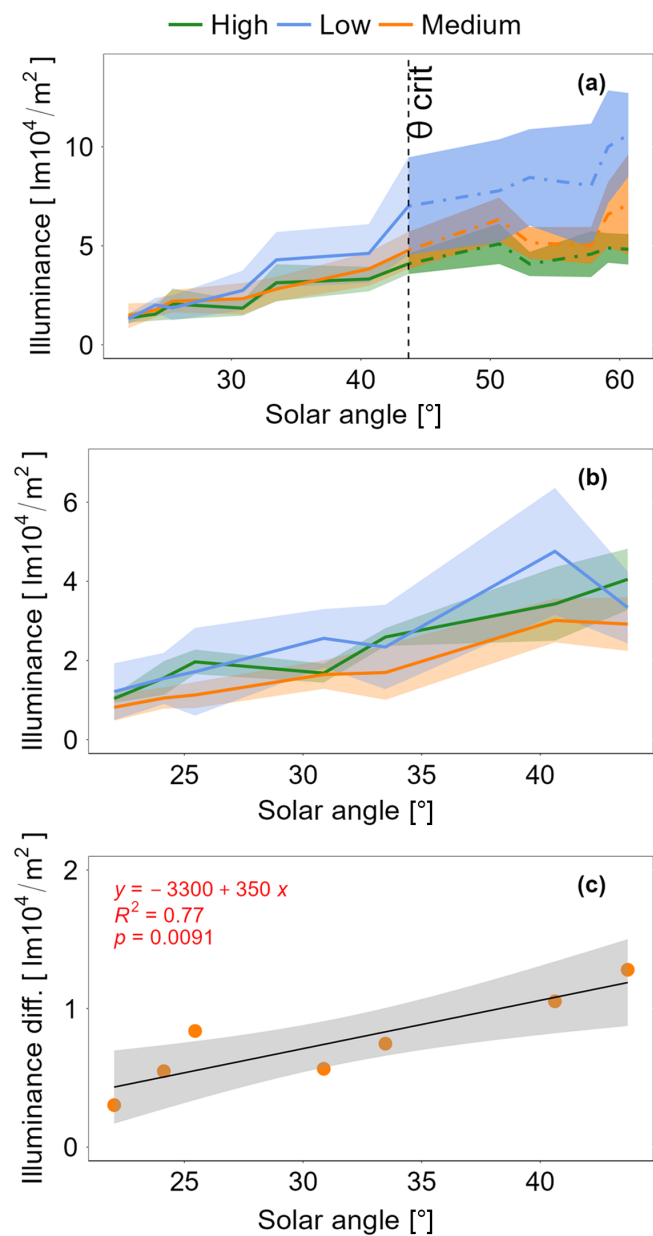


FIGURE 5 Illuminance versus solar altitude angle in (a) high sensors and (b) low sensors, but only below the critical solar altitude angle reported in (a). (c) Difference of illuminance between high and low sensors in the mid-sites where shrubs are more abundant than *Phragmites*. Colored shaded areas in (a) and (b) describe the range of data around the mean. Gray-shaded areas in (c) identify the 95% CI of linear regression.

biomass value was as high as the value calculated in the low forest site L6 (between 25 and 125 g/m^2), the temperature values were between 4% (M2_2-L6_1) to 7% (M2_1-L6_2) lower. A similar difference can be seen between H7, mostly dominated by *Phragmites*, and M1, mostly dominated by *M. cerifera*. On the other side, the highest illuminance reduction can be found in M2, where values are between 14% and 25% lower than L6 (Figure 7c).

DISCUSSION

Monthly illuminance and temperature were significantly different across a transect perpendicular to the marsh-forest boundary. In particular, high sensors located at 2 m above the ground surface allowed quantification of light attenuation by the tree canopy, while low sensors at 30 cm effectively described the understory shrub effect in intercepting solar radiation penetrating the tree canopy. Although the analysis was carried out on a dataset limited both in space and time, the results obtained are encouraging and can be used to characterize light dynamics along a coastal forest-marsh gradient. Future research will estimate changes in light patterns over time during forest retreat. The results are concisely summarized in Figure 8.

Light interception: Tree canopy and understory vegetation

The light environment is strongly influenced by canopy and understory light capture (Messier et al., 1998). In our data, healthy tree canopies reduced illuminance values by 40%–54%, while understory vegetation absorbed 23%–45% of the transmitted light. We found that a major factor in the attenuation of understory light was the abundance of *M. cerifera*. Differences between tree and understory vegetation attenuation were further related to LAI, intra-leaf shading effects, and leaf angle differences as we describe in more detail below.

LAI is essential to the estimation of light attenuation due to canopies. According to Duursma and Mäkelä (2007), in idealized single tree's light interception depends on total crown size and increases as leaf area increases. Larger crowns have less self-shading effects; thus, light interception per unit of leaf area is higher. In experiments carried out on unmanaged *Pinus contorta* forests in the Rocky Mountains, Sampson and Smith (1993) showed the chief role that LAI plays in light penetration, followed by foliage aggregation, average leaf inclination angle, and vertical distribution of foliage. In particular, their measurements suggested that the extinction coefficient (measuring light attenuation through a medium) decreased from 0.70 to 0.28 as LAI increased from 1.5 to 4.5, due to foliage overlapping and foliage self-shading. Heterogeneous canopies are characterized by open gaps, facilitating light penetration in the forest understory (Duursma & Mäkelä, 2007; Ni et al., 1997). Light penetrating through gaps can encourage photosynthetic activity of understory vegetation. Sensors placed in the understory of a coniferous and broadleaf forest showed that light transmittance during the growing season increases with gap fraction, according to a factor of

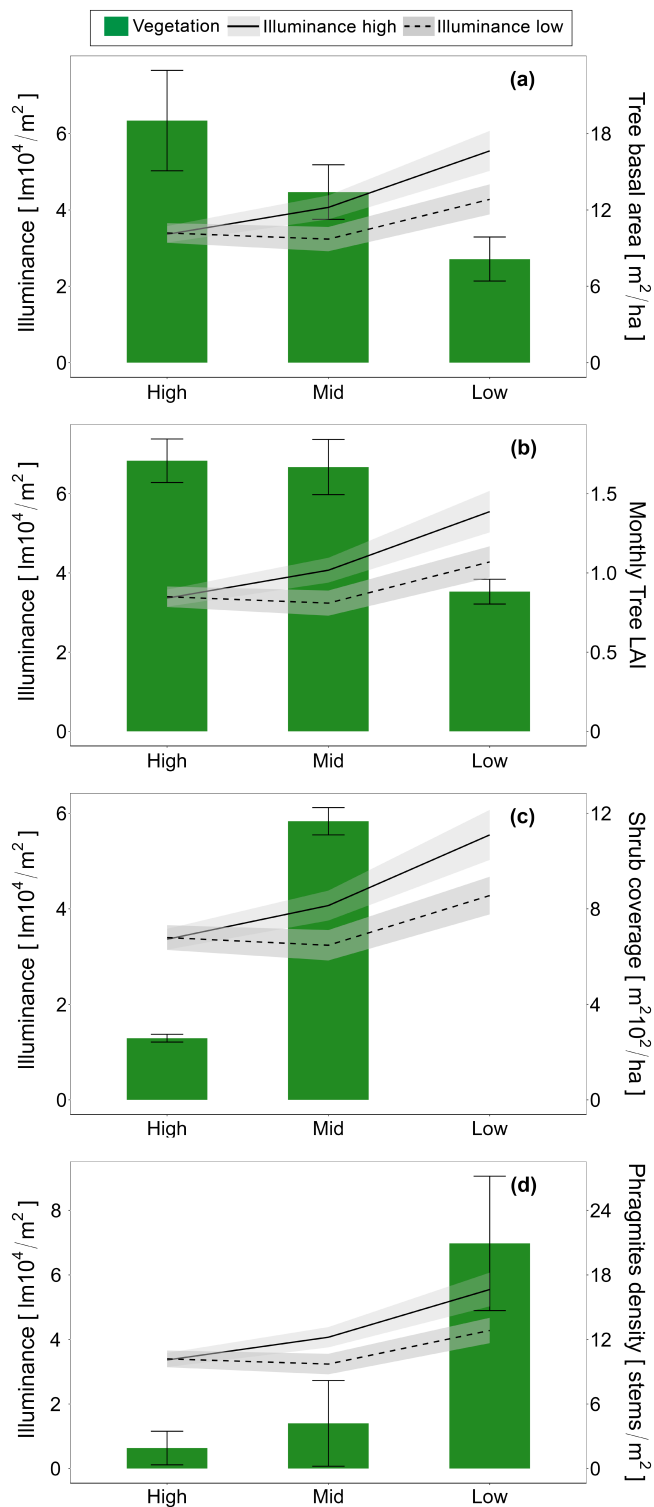


FIGURE 6 Illuminance variability over the forest in both high (solid black line) and low sensors (dotted black line) compared with (a) tree basal area, (b) monthly mean tree leaf area index (LAI), (c) shrub basal area, and (d) *Phragmites australis* percentage cover. Gray areas describe the range of data around the mean.

1.33 (Comeau, 2000). Light interception is higher in the high forest, since trees have larger basal area and higher LAI (Kashian et al., 2005). In our study site, where tree

crowns are large and the canopy is not dense, light interception is high when LAI is high, and the shading effect of foliage is weak. In the low forest sites, LAI was minimal, many tree canopies were barren, and light reached the high sensors with little attenuation.

Our results agree with those of Martens et al. (2000), who simulated understory light in a grassland/forest continuum in plots with isolated or aggregated tree configurations and variable tree heights and canopy covers. They showed that transmitted photosynthetically active radiation decreased when the percentage cover in the continuum increased from 0 to 81%. Moreover, they suggested that understory light in inter-canopy plots (gaps) was less variable than in canopy plots and that tree height decreased the transmitted radiation to the understory.

Light transmitted to the understory is intercepted and attenuated by the tallest understory vegetation. We observed a shading effect of tall understory species like shrubs and *Ph. australis*, which would likely inhibit the colonization and growth of other herbaceous and short stature species. According to Brantley and Young (2007), *M. cerifera* is characterized by high LAI that significantly reduces the light penetration in shrub thickets. They estimated LAI values in young stands between 9.8 and 12.5 m^2/m in a shrub area in Hog Island Bay. We estimated the effect of *M. cerifera* shrubs by quantifying reductions in light penetration over the seasons. Here the maximum light attenuation of around 45% was reached in fall, when *M. cerifera* biomass reached its peak (Griffin & Blazich, 2008). In the low forest *Ph. australis* is abundant, with very few other species. The presence of only two understory plants underscores the high stress level triggered by salinity and frequent flooding. In a different environment richer in understory species, the light attenuation would be affected by the variable shading, attenuation, and reflection of each plant. Illuminance values are therefore a function of biodiversity richness, physical characteristics of vegetation species, and their health state. However, we would expect to see a similar general trend, with less understory vegetation and related attenuation in the healthy forest and more understory vegetation and attenuation in the disturbed forest.

Light attenuation varies with seasons. During the growing season, vegetation stems and leaves reduce transmitted light. This effect is weaker in the non-determining what new vegetation species can encroach in this area growing season when leaf area is reduced. Although *Pi. taeda* is an evergreen, its growing season is in spring and summer; *Ph. australis* peak growth is between June and September; *M. cerifera* blooms in spring and sets seed in summer, reaching peak biomass in fall (Griffin & Blazich, 2008). Therefore, we generally expected and observed maximal tree canopy

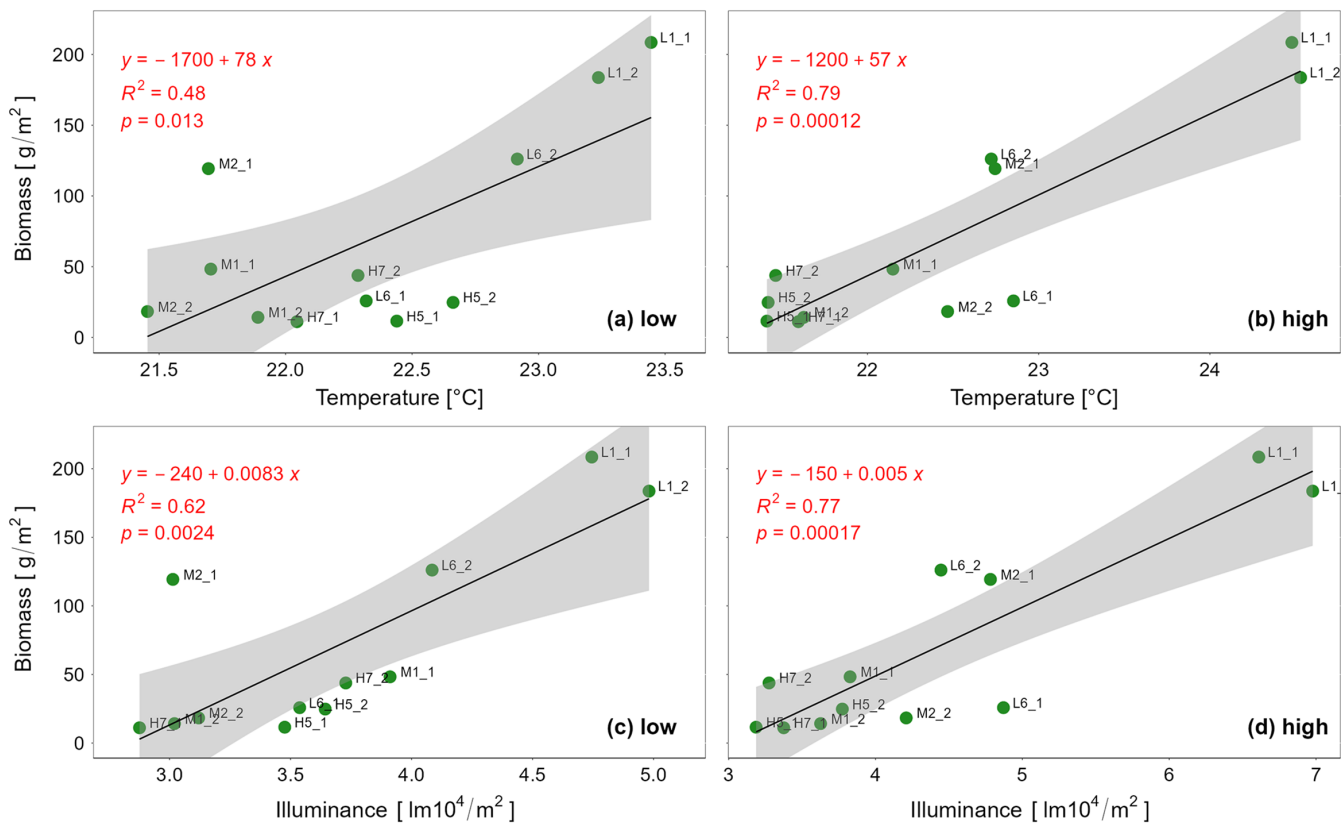


FIGURE 7 Linear regression model between average (a, b) temperature, (c, d) illuminance, and vegetation understory biomass calculated for each site, for the high and low sensors. Gray-shaded areas identify the 95% CI of linear regression.

attenuation in spring and summer, and maximal understory attenuation in fall.

Light transmission to understory varies over the months depending on solar elevation angle. Using quantum sensor measurements and fish-eye photographs Canham et al. (1994) found that light transmission is higher for higher solar elevation angles due to the large canopy openness overhead, with short light path length through crowns. For angles closer to the horizon, light transmission is limited due to leaf interception. They also showed that at latitudes of ~39° N–42° N, most radiation overhead originated from solar angles ranging from 15° N to 50° N from the zenith (~40°–75° elevation). Canham et al. (1999) further showed that at higher latitudes (55° N) canopy openness directly overhead was between 20% and 70%, and that most light transmission to the understory originated for solar angles ranging from 35° to 60° from the horizon. Canham et al. (1994) also reported that for different closed forested stand types, the gap light index (the percentage of light transmitted to the understory vegetation excluding the beam enrichment) ranged from the 0.5 to 5 at 1 m height beneath the tree canopy, while from 0.5 to 8 at the ground level. Trentini et al. (2017) measured light transmission in a *Pi. taeda* forest in Argentina, characterized by different canopy openness. They showed that for

canopy openness variable from 8% to 14% the light transmitted to the understory varied from 15% to 25%. Our results partially confirm those presented in Canham et al. (1994) in temperate forests at similar latitudes. In our study site, light transmission to understory vegetation occurs for solar elevation angles ranging from ~22° (68° from zenith) in December to ~60° (30° from zenith) in June, with maximum values reached for angle higher than $\theta_{crit} = 43^\circ$ (30°–47° from the zenith). Here, the percentage of light measured at 2 m above the ground surface is between 45% and 76%, respectively, in high and low forests (Figure 8). For angles lower than θ_{crit} , a significant difference between light transmission in high, mid-; Nordio et al. 2023, and low forests was not detected. For angles higher than this threshold, light transmission in the low forest was much higher. We think that this difference is the result of both variations in canopy structure and edge effects at the forest-marsh boundary. In the low forest, light penetrates laterally from the marsh and compounds with higher penetration overhead due to canopy dieback. Walters et al. (2021) carried out a 5-year field experiment to simulate a natural disturbance event by inducing the death of established *Pi. taeda* trees. In their experiment, the light level was consistently low in control plots in the high forest (characterized by intact tree canopies) with an attenuation

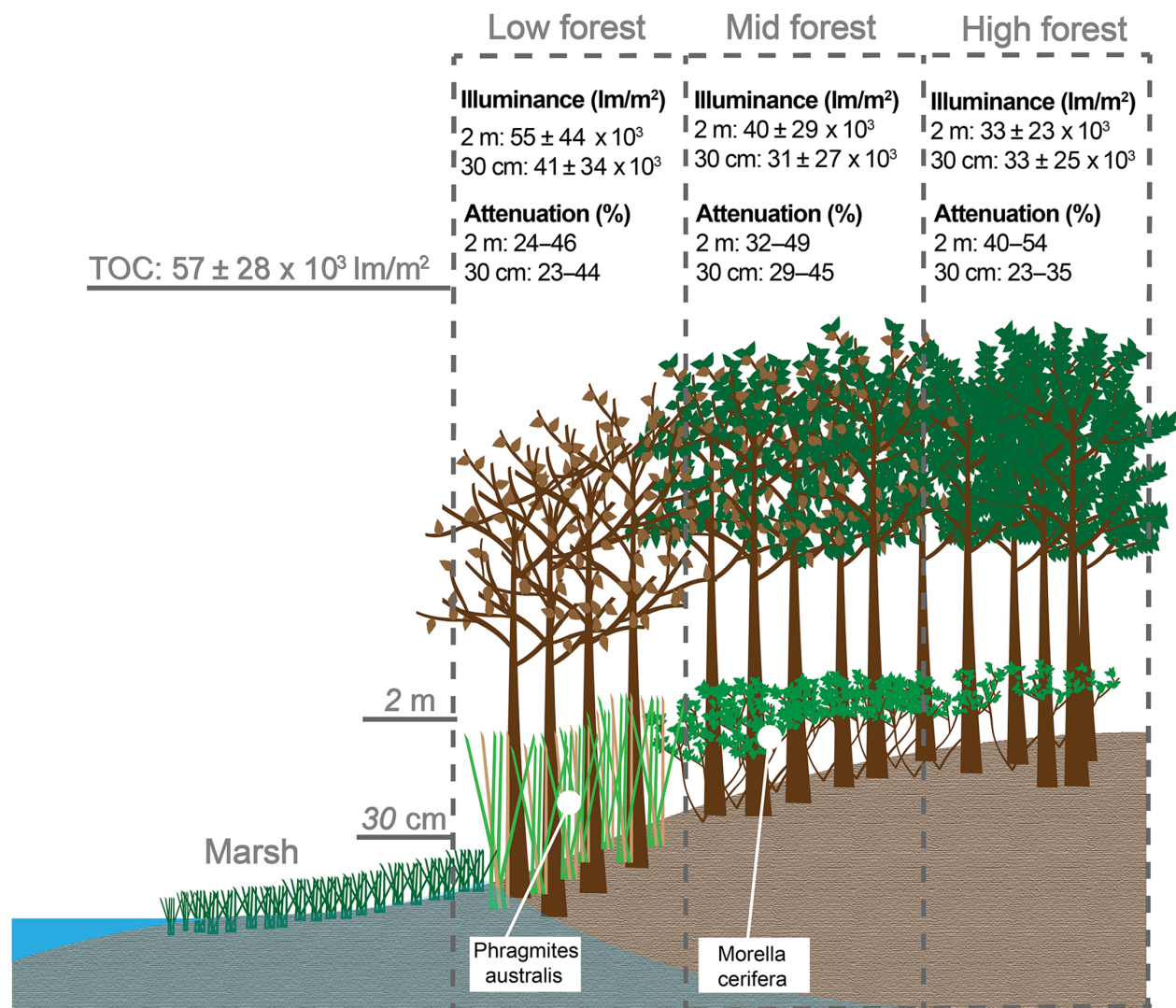


FIGURE 8 Summary of illuminance and attenuation values due to tree canopy and understory vegetation in the different forested sites. The forest is dominated by *Pinus taeda*. The trees are healthy in the high forest and barren or dead in the low forest.

of ~80%. In the low and transition areas closer to the marsh, the light attenuation was between 70% and 60%. Through this study, we want to confirm the results obtained in Walters et al. (2021) and provide a quantitative assessment of the light conditions along this ecotone. To determine how much light is available along the forest-marsh boundary determining what new vegetation species can encroach in this area is very important. Moreover, these data are fundamental for ecological models of forest retreat. We therefore believe that our data are of great use for the scientific community.

Temperature and understory vegetation

Even if no significant differences were found in the temperature values measured at 30 cm above the ground

surface, values in the mid-forest tended to be lower than those in the high and low forest. Woodland vegetation can modify the temperature regime, creating a microclimate. In particular, beneath the forest canopy, ambient temperatures exhibit a lower maximum and a milder minimum relative to forest gaps. Canopies provide a sheltering effect for understory vegetation by reducing seedling exposure to intense radiation and radiative cooling at night (D'Odorico et al., 2010, 2013). Huang et al. (2018) characterized the microclimate produced by *M. cerifera* in a grassland. Below *M. cerifera* shrubs, daily temperatures over the year were lower than in the grassland, while during the nighttime, temperatures tended to be higher. In shaded areas, evapotranspiration was 1.6 times lower and temperature 6.4°C lower than in unshaded areas (Webster & Day, 1993). Lower evapotranspiration may limit soil salinization (Salama et al., 1999), positively

influencing species with low-salt tolerance. This effect could slightly temper the larger, negative effect of shading by *M. cerifera* on understory species.

Light penetration and *Ph. australis* encroachment: Edge effects

Light data coupled with vegetation data confirm forest transgression and consequent marsh expansion in the study site, describing the different successional stages of forest-marsh transition. In the low forest, maximum values of illuminance and temperature were reached during summer. The forest-marsh edge is essential in terms of enhanced light penetration in the forest. This effect was observed in the low forest, where high light availability was the product of vertical and lateral light transmission. Light and temperature, the main drivers of photosynthetic activity, promote growth of established vegetation and the invasion of new species (Jobe IV & Gedan, 2021). *Ph. australis* is the most common invasive species in the North Atlantic coastal forests where flooding events are frequent. *Ph. australis* often represents the first stage of forest conversion to salt marsh, before marsh vegetation establishes in the dieback area. A recent study conducted in Chesapeake Bay (VA) suggested that although *Ph. australis* could survive in low-light environments, the species thrives in high-light conditions (Shaw et al., 2022). Maximum illuminance values reached in the low-forest sites explain the large percentage cover of *Ph. australis*. At the same time, the presence of this species in site H7, where illuminance values are low, confirms that *Ph. australis* can also colonize shaded areas, as indicated by Shaw et al. (2022). In the low forest, we observed almost exclusive dominance of this species. Data collected at 30 cm show a significant attenuation of light by *Ph. australis* compared with sensors at 2 m, a finding which also agrees with prior observations (Chambers et al., 1999; Hirtreiter & Potts, 2012).

Light availability and climate change

Light availability along the marsh-forest ecotone is crucial for the expansion of invasive vegetation and the establishment of marsh vegetation (Zhu et al., 2003). The health state of trees and the canopy architecture influence the light transmission to understory vegetation (Canham et al., 1994), suggesting different light patterns along the forest-marsh gradient. At the marsh-forest boundary, where salinization and flooding events are frequent, high illuminance to the understory vegetation increases soil salinity through high evaporation. This leads

to additional canopy loss and inhibits the establishment of tree seedlings (Kurz & Wagner, 1957). On the other hand, new invasive species can facilitate tree germination and sapling regrowth, decreasing soil moisture conditions and groundwater tables where soil salinity conditions are tolerable (Poulter et al., 2008). Higher illuminance from the marsh edge contributes little to evaporation in the low forest, where higher illuminance due to canopy dieback dominates (Zhu et al., 2003), but can be beneficial for sapling regrowth in inland areas, where salinity and inundation level are moderate (Nordio et al., 2024). *Ph. australis* prefers high illuminance zones with high temperatures (Ekstam et al., 1999) and expands in areas closer to the forest-marsh edge (Jobe IV & Gedan, 2021; Shaw et al., 2022).

Recent work in ghost forests suggested that forest retreat and marsh expansion may encourage large net carbon emissions due to biomass mortality that is offset in the short-term by increased soil carbon sequestration in the new marshes, causing the coastal area to convert to a carbon source (Kirwan et al., 2023; Warnell et al., 2022).

CONCLUSIONS

Overall, our results quantified the spatial and temporal variability of illuminance and temperature along the healthy-ghost forest continuum, shedding light on the processes governing coastal forest retreat due to salinization and flooding. In the healthy forest, where trees are characterized by large basal area, the tree canopy intercepts a large fraction of available light. For solar angles higher than 43°, monthly mean illuminance significantly differs in high, mid-, and low forests. A slightly higher maximum illuminance in the mid-forest can be justified by lateral light penetration (edge effect). In the low forest, closer to the marsh, light penetration is due to the combination of edge effect and canopy thinning. Light attenuation by *M. cerifera*, was between 29% and 45% in the mid-forest while the shading effect of *Ph. australis* peaked at 44% during the growing season. Minimal attenuation occurred in the low forest due to canopy thinning. Lateral penetration of light encouraged the expansion of *Ph. australis*, representing the first step of forest retreat. In the mid-forest, the effect of denser *M. cerifera* canopies lowers temperatures collected at 30 cm below the ground surface of around 4%–6.5% in comparison with high forest and low forest. This mitigating effect encourages the establishment of new microclimates.

ACKNOWLEDGMENTS

This research was funded by the USA National Science Foundation awards 1832221 (VCR-LTER) and 2012322 (CZN Coastal Critical Zone).

CONFLICT OF INTEREST STATEMENT

The authors declare no conflicts of interest.

DATA AVAILABILITY STATEMENT

Data (Fagherazzi & Nordio, 2022; Gedan et al., 2021) are available from the EDI Data Portal: <https://doi.org/10.6073/pasta/942a5a981e6e986c5fa1a9a9cd2eb8b7> and <https://doi.org/10.6073/pasta/f5d6779021676538649c445dc3a4fbf7>, respectively.

ORCID

Giovanna Nordio  <https://orcid.org/0000-0002-4133-4985>

Keryn Gedan  <https://orcid.org/0000-0003-4020-5441>

REFERENCES

Antonellini, M., and P. N. Mollema. 2010. "Impact of Groundwater Salinity on Vegetation Species Richness in the Coastal Pine Forests and Wetlands of Ravenna, Italy." *Ecological Engineering* 36(9): 1201–11.

Beaudet, M., C. Messier, and A. Leduc. 2004. "Understorey Light Profiles in Temperate Deciduous Forests: Recovery Process Following Selection Cutting." *Journal of Ecology* 92(2): 328–338.

Becker, P., and A. P. Smith. 1990. "Spatial Autocorrelation of Solar Radiation in a Tropical Moist Forest Understory." *Agricultural and Forest Meteorology* 52(3–4): 373–79.

Brantley, S. T., and D. R. Young. 2007. "Leaf-Area Index and Light Attenuation in Rapidly Expanding Shrub Thickets." *Ecology* 88(2): 524–530.

Canham, C. D. 1988. "An Index for Understory Light Levels in and around Canopy Gaps." *Ecology* 69(5): 1634–38.

Canham, C. D., A. C. Finzi, S. W. Pacala, and D. H. Burbank. 1994. "Causes and Consequences of Resource Heterogeneity in Forests: Interspecific Variation in Light Transmission by Canopy Trees." *Canadian Journal of Forest Research* 24(2): 337–349.

Canham, C. D., J. S. Denslow, W. J. Platt, J. R. Runkle, T. A. Spies, and P. S. White. 1990. "Light Regimes beneath Closed Canopies and Tree-Fall Gaps in Temperate and Tropical Forests." *Canadian Journal of Forest Research* 20(5): 620–631.

Canham, C. D., K. D. Coates, P. Bartemucci, and S. Quaglia. 1999. "Measurement and Modeling of Spatially Explicit Variation in Light Transmission through Interior Cedar-Hemlock Forests of British Columbia." *Canadian Journal of Forest Research* 29(11): 1775–83.

Carr, J., G. Guntenspergen, and M. Kirwan. 2020. "Modeling Marsh-Forest Boundary Transgression in Response to Storms and Sea-Level Rise." *Geophysical Research Letters* 47(17): e2020GL088998.

Chambers, R. M., L. A. Meyerson, and K. Saltonstall. 1999. "Expansion of *Phragmites australis* into Tidal Wetlands of North America." *Aquatic Botany* 64(3–4): 261–273.

Comeau, P. 2000. Measuring Light in the Forest. No. 42. doi:10.13140/RG.2.1.3225.3525

Conner, W. H., T. W. Doyle, and K. W. Krauss, eds. 2007. *Ecology of Tidal Freshwater Forested Wetlands of the Southeastern United States* 448–450. Dordrecht: Springer.

D'Odorico, P., J. D. Fuentes, W. T. Pockman, S. L. Collins, Y. He, J. S. Medeiros, S. DeWekker, and M. E. Litvak. 2010. "Positive Feedback between Microclimate and Shrub Encroachment in the Northern Chihuahuan Desert." *Ecosphere* 1(6): 1–11.

D'Odorico, P., Y. He, S. Collins, S. F. De Wekker, V. Engel, and J. D. Fuentes. 2013. "Vegetation–Microclimate Feedbacks in Woodland–Grassland Ecotones." *Global Ecology and Biogeography* 22(4): 364–379.

Dale, M. R., and M. J. Fortin. 2009. "Spatial Autocorrelation and Statistical Tests: Some Solutions." *Journal of Agricultural, Biological, and Environmental Statistics* 14: 188–206.

Delgado, J. D., N. L. Arroyo, J. R. Arévalo, and J. M. Fernández-Palacios. 2007. "Edge Effects of Roads on Temperature, Light, Canopy Cover, and Canopy Height in Laurel and Pine Forests (Tenerife, Canary Islands)." *Landscape and Urban Planning* 81(4): 328–340.

Desantis, L. R., S. Bhotika, K. Williams, and F. E. Putz. 2007. "Sea-Level Rise and Drought Interactions Accelerate Forest Decline on the Gulf Coast of Florida, USA." *Global Change Biology* 13(11): 2349–60.

Dormann, C. F., M. Bagnara, S. Boch, J. Hinderling, A. Janeiro-Otero, D. Schäfer, P. Schall, and F. Hartig. 2020. "Plant Species Richness Increases with Light Availability, but Not Variability, in Temperate Forests Understorey." *BMC Ecology* 20(1): 1–9.

Doyle, T. W., K. W. Krauss, W. H. Conner, and A. S. From. 2010. "Predicting the Retreat and Migration of Tidal Forests along the Northern Gulf of Mexico under Sea-Level Rise." *Forest Ecology and Management* 259(4): 770–77.

Duursma, R. A., and A. Mäkelä. 2007. "Summary Models for Light Interception and Light-Use Efficiency of Non-Homogeneous Canopies." *Tree Physiology* 27(6): 859–870.

Ekstam, B., R. Johannesson, and P. Milberg. 1999. "The Effect of Light and Number of Diurnal Temperature Fluctuations on Germination of *Phragmites Australis*." *Seed Science Research* 9(2): 165–170.

Fagherazzi, S., G. Nordio, K. Munz, D. Catucci, and W. S. Kearney. 2019. "Variations in Persistence and Regenerative Zones in Coastal Forests Triggered by Sea Level Rise and Storms." *Remote Sensing* 11(17): 2019.

Fagherazzi, S., and G. Nordio. 2022. "Groundwater, Soil Moisture, Light and Weather Data in Brownsville Forest, Nassawadox, VA, 2019–2022. Knb-Lter-Vcr.349.4." In *Environmental Data Initiative. Dataset. VCR-LTER* website <https://doi.org/10.6073/pasta/942a5a981e6e986c5fa1a9a9cd2eb8b7>.

Field, C. R., C. Gjerdrum, and C. S. Elphick. 2016. "Forest Resistance to Sea-Level Rise Prevents Landward Migration of Tidal Marsh." *Biological Conservation* 201: 363–69.

Gedan, K., J. MacGregor, R. Mohammadi, and A. Khan. 2021. "Forest Transition Experiment – Vegetation Monitoring on a Coastal Virginia Forest, 2019–2021. Knb-Lter-Vcr.361.3." Environmental Data Initiative. Dataset. <https://doi.org/10.6073/pasta/f5d6779021676538649c445dc3a4fbf7>.

Griffin, J. J., and F. A. Blazich. 2008. *Myrica L. and Morella Lour. Woody Plant Seed Manual* 733–37. Washington DC: USDA Forest Service.

Gu, L., J. D. Fuentes, M. Garstang, J. T. Da Silva, R. Heitz, J. Sigler, and H. H. Shugart. 2001. "Cloud Modulation of Surface Solar

Irradiance at a Pasture Site in Southern Brazil." *Agricultural and Forest Meteorology* 106(2): 117–129.

Haaf, L., S. F. Dymond, and D. A. Kreeger. 2021. "Principal Factors Influencing Tree Growth in Low-Lying Mid Atlantic Coastal Forests." *Forests* 12(10): 1351.

Hirtreiter, J. N., and D. L. Potts. 2012. "Canopy Structure, Photosynthetic Capacity and Nitrogen Distribution in Adjacent Mixed and Monospecific Stands of *Phragmites australis* and *Typha latifolia*." *Plant Ecology* 213(5): 821–29.

Huang, H., J. C. Zinnert, L. K. Wood, D. R. Young, and P. D'Odorico. 2018. "Non-Linear Shift from Grassland to Shrubland in Temperate Barrier Islands." *Ecology* 99(7): 1671–81.

Hutchison, B. A., and D. R. Matt. 1976. "Beam Enrichment of Diffuse Radiation in a Deciduous Forest." *Agricultural Meteorology* 17(2): 93–110.

Jobe, J. G. D., IV, and K. Gedan. 2021. "Species-Specific Responses of a Marsh-Forest Ecotone Plant Community Responding to Climate Change." *Ecology* 102(4): e03296.

Johnson, S. R., and D. R. Young. 1993. "Factors Contributing to the Decline of *Pinus taeda* on a Virginia Barrier Island." *Bulletin of the Torrey Botanical Club* 120: 431–38.

Jolly, I. D., G. R. Walker, and P. J. Thorburn. 1993. "Salt Accumulation in Semi-Arid Floodplain Soils with Implications for Forest Health." *Journal of Hydrology* 150(2-4): 589–614.

Kashian, D. M., M. G. Turner, and W. H. Romme. 2005. "Variability in Leaf Area and Stemwood Increment along a 300-Year Lodgepole Pine Chronosequence." *Ecosystems* 8(1): 48–61.

Kauppi, P., J. Selkäinaho, and P. Puttonen. 1983. "A Method for Estimating above-Ground Biomass in *Phragmites* Stands." *Annales Botanici Fennici* 20: 51–55.

Kearney, W. S., A. Fernandes, and S. Fagherazzi. 2019. "Sea-Level Rise and Storm Surges Structure Coastal Forests into Persistence and Regeneration Niches." *PLoS One* 14(5): e0215977.

Kirwan, M. L., J. P. Megonigal, G. L. Noyce, and A. J. Smith. 2023. "Geomorphic and Ecological Constraints on the Coastal Carbon Sink." *Nature Reviews Earth & Environment* 4(6): 393–406.

Kirwan, M. L., and K. B. Gedan. 2019. "Sea-Level Driven Land Conversion and the Formation of Ghost Forests." *Nature Climate Change* 9(6): 450–57.

Kotuby-Amacher, J., R. Koenig, and B. Kitchen. 2000. *Salinity and Plant Tolerance*. Logan, UT: Electronic Publication AG-SO-03, Utah State University Extension.

Kurz, H., and K. A. Wagner. 1957. *Tidal Marshes of the Gulf and Atlantic Coasts of Northern Florida and Charleston, South Carolina*. Tallahassee, FL: Florida State University.

Lieffers, V. J., C. Messier, K. J. Stadt, F. Gendron, and P. G. Comeau. 1999. "Predicting and Managing Light in the Understory of Boreal Forests." *Canadian journal of forest research* 29(6): 796–811.

Long, M. H., J. E. Rheuban, P. Berg, and J. C. Zieman. 2012. "A Comparison and Correction of Light Intensity Loggers to Photosynthetically Active Radiation Sensors." *Limnology and Oceanography: Methods* 10(6): 416–424.

Martens, S. N., D. D. Breshears, and C. W. Meyer. 2000. "Spatial Distributions of Understory Light along the Grassland/Forest Continuum: Effects of Cover, Height, and Spatial Pattern of Tree Canopies." *Ecological Modelling* 126(1): 79–93.

McDowell, N. G., M. Ball, B. Bond-Lamberty, M. L. Kirwan, K. W. Krauss, J. P. Megonigal, M. Mencuccini, N. D. Ward, N. M. Weintraub, and V. Bailey. 2022. "Processes and Mechanisms of Coastal Woody-Plant Mortality." *Global Change Biology* 28 (20): 5881–5900.

Messier, C., S. Parent, and Y. Bergeron. 1998. "Effects of Overstory and Understory Vegetation on the Understory Light Environment in Mixed Boreal Forests." *Journal of Vegetation Science* 9(4): 511–520.

Michael, P. R., D. E. Johnston, and W. Moreno. 2020. "A Conversion Guide: Solar Irradiance and Lux Illuminance." *Journal of Measurements in Engineering* 8(4): 153–166.

Monteith, J., and M. Unsworth. 2013. *Principles of Environmental Physics: Plants, Animals, and the Atmosphere*. Oxford, UK: Academic Press.

Montgomery, R. A., and R. L. Chazdon. 2001. "Forest Structure, Canopy Architecture, and Light Transmittance in Tropical Wet Forests." *Ecology* 82(10): 2707–18.

Munns, R., and M. Tester. 2008. "Mechanisms of Salinity Tolerance." *Annual Review of Plant Biology* 59: 651–681.

Ni, W., X. Li, C. E. Woodcock, J. L. Roujeau, and R. E. Davis. 1997. "Transmission of Solar Radiation in Boreal Conifer Forests: Measurements and Models." *Journal of Geophysical Research: Atmospheres* 102(D24): 29555–66.

Nicotra, A. B., R. L. Chazdon, and S. V. Iriarte. 1999. "Spatial Heterogeneity of Light and Woody Seedling Regeneration in Tropical Wet Forests." *Ecology* 80(6): 1908–26.

Nordio, G., K. Gedan, and S. Fagherazzi. 2024. "Storm Surges and Sea Level Rise Cluster Hydrological Variables Across a Coastal Forest Bordering a Salt Marsh." *Water Resources Research* 60(2): e2022WR033931.

Nordio, G., R. Frederiks, M. Hingst, J. Carr, M. Kirwan, K. Gedan, H. Michael, and S. Fagherazzi. 2023. "Frequent Storm Surges Affect the Groundwater of Coastal Ecosystems." *Geophysical Research Letters* 50(1): e2022GL100191.

Nordio, G., and S. Fagherazzi. 2022. "Groundwater, Soil Moisture, Light and Weather Data Collected in a Coastal Forest Bordering a Salt Marsh in the Delmarva Peninsula (VA)." *Data in Brief* 108584: 108584.

Pezeshki, S. R. 1992. "Response of *Pinus taeda* L to Soil Flooding and Salinity." *Annales des Sciences Forestières* 49(2): 149–159.

Pohlman, C. L., S. M. Turton, and M. Goosem. 2007. "Edge Effects of Linear Canopy Openings on Tropical Rain Forest Understory Microclimate." *Biotropica* 39(1): 62–71.

Porter, J. H., D. O. Krovetz, W. K. Nuttle, and J. Spitler. 2022. "Hourly Meteorological Data for the Virginia Coast Reserve LTER 1989-Present." Virginia Coast Reserve Long-Term Ecological Research Project Data Publication knb-lter-vcr.25.47. <https://doi.org/10.6073/pasta/3d24e9016862e74f7e7b56b991e67925>.

Poulter, B., N. L. Christensen, and S. S. Qian. 2008. "Tolerance of *Pinus taeda* and *Pinus serotina* to low salinity and flooding: Implications for equilibrium vegetation dynamics." *Journal of Vegetation Science* 19(1): 15–22.

Raz-Yaseef, N., E. Rotenberg, and D. Yakir. 2010. "Effects of Spatial Variations in Soil Evaporation Caused by Tree Shading on Water Flux Partitioning in a Semi-Arid Pine Forest." *Agricultural and Forest Meteorology* 150(3): 454–462.

Rissanen, K., M. O. Martin-Guay, A. S. Riopel-Bouvier, and A. Paquette. 2019. "Light Interception in Experimental Forests Affected by Tree Diversity and Structural Complexity of Dominant Canopy." *Agricultural and Forest Meteorology* 278: 107655.

Rosema, A., W. Verhoef, H. Noorbergen, and J. J. Borgesius. 1992. "A New Forest Light Interaction Model in Support of Forest Monitoring." *Remote Sensing of Environment* 42(1): 23–41.

Sah, J. P., M. S. Ross, S. Koptur, and J. R. Snyder. 2004. "Estimating Aboveground Biomass of Broadleaved Woody Plants in the Understory of Florida Keys Pine Forests." *Forest Ecology and Management* 203(1–3): 319–329.

Salama, R. B., C. J. Otto, and R. W. Fitzpatrick. 1999. "Contributions of Groundwater Conditions to Soil and Water Salinization." *Hydrogeology Journal* 7(1): 46–64.

Sampson, D. A., and F. W. Smith. 1993. "Influence of Canopy Architecture on Light Penetration in Lodgepole Pine (*Pinus contorta* var. *latifolia*) Forests." *Agricultural and Forest Meteorology* 64(1–2): 63–79.

Schieder, N. W., and M. L. Kirwan. 2019. "Sea-Level Driven Acceleration in Coastal Forest Retreat." *Geology* 47(12): 1151–55.

Shaw, P., J. Jobe, and K. B. Gedan. 2022. "Environmental Limits on the Spread of Invasive *Phragmites australis* into Upland Forests with Marine Transgression." *Estuaries and Coasts* 45(2): 539–550.

Smith, J. A. 2013. "The Role of *Phragmites australis* in Mediating Inland Salt Marsh Migration in a Mid-Atlantic Estuary." *PLoS One* 8(5): e65091.

Stenberg, P. 1996. "Simulations of the Effects of Shoot Structure and Orientation on Vertical Gradients in Intercepted Light by Conifer Canopies." *Tree Physiology* 16(1–2): 99–108.

Stickley, S. F., and J. M. Fraterrigo. 2021. "Understory Vegetation Contributes to Microclimatic Buffering of Near-Surface Temperatures in Temperate Deciduous Forests." *Landscape Ecology* 36: 1197–1213.

Tang, L., D. Yin, C. Chen, D. Yu, and W. Han. 2019. "Optimal Design of Plant Canopy Based on Light Interception: A Case Study with Loquat." *Frontiers in Plant Science* 10: 364.

Trentini, C. P., P. I. Campanello, M. Villagra, L. Ritter, A. Ares, and G. Goldstein. 2017. "Thinning of Loblolly Pine Plantations in Subtropical Argentina: Impact on Microclimate and Understory Vegetation." *Forest Ecology and Management* 384: 236–247.

Tully, K., K. Gedan, R. Epanchin-Niell, A. Strong, E. S. Bernhardt, T. BenDor, M. Mitchell, et al. 2019. "The Invisible Flood: The Chemistry, Ecology, and Social Implications of Coastal Saltwater Intrusion." *BioScience* 69(5): 368–378.

Wagner, H. H., and M. J. Fortin. 2005. "Spatial Analysis of Landscapes: Concepts and Statistics." *Ecology* 86(8): 1975–87.

Walters, D. C., J. A. Carr, and M. L. Kirwan. 2021. "Experimental Tree Mortality Does Not Induce Marsh Transgression in a Chesapeake Bay Low-Lying Coastal Forest." *Frontiers in Marine Science* 8: 782643.

Warnell, K., L. Olander, and C. Currin. 2022. "Sea Level Rise Drives Carbon and Habitat Loss in the US Mid-Atlantic Coastal Zone." *PLoS Climate* 1(6): e0000044.

Webster, I. T., and C. R. B. Day. 1993. "The Impacts of Shade on Evaporation Rates and Temperatures in Stock Watering Troughs." *Australian Journal of Agricultural Research* 44(2): 287–298.

Whitmore, T. 1989. "Canopy Gaps and the Two Major Groups of Forest Trees." *Ecology* 70(3): 536–38.

Williams, K., K. C. Ewel, R. P. Stumpf, F. E. Putz, and T. W. Workman. 1999. "Sea-Level Rise and Coastal Forest Retreat on the West Coast of Florida, USA." *Ecology* 80(6): 2045–63.

Woods, N. N., J. L. Swall, and J. C. Zinnert. 2020. "Soil Salinity Impacts Future Community Composition of Coastal Forests." *Wetlands* 40(5): 1495–1503.

Yamamoto, S. I. 2000. "Forest Gap Dynamics and Tree Regeneration." *Journal of Forest Research* 5: 223–29.

Zhu, J. J., T. Matsuzaki, F. Q. Lee, and Y. Gonda. 2003. "Effect of Gap Size Created by Thinning on Seedling Emergency, Survival and Establishment in a Coastal Pine Forest." *Forest Ecology and Management* 182(1–3): 339–354.

SUPPORTING INFORMATION

Additional supporting information can be found online in the Supporting Information section at the end of this article.

How to cite this article: Nordio, Giovanna, Keryn Gedan, and Sergio Fagherazzi. 2024. "Shifts in Light Availability Driven by Dieback across a Marsh-Forest Gradient." *Ecosphere* 15(10): e70021. <https://doi.org/10.1002/ecs2.70021>